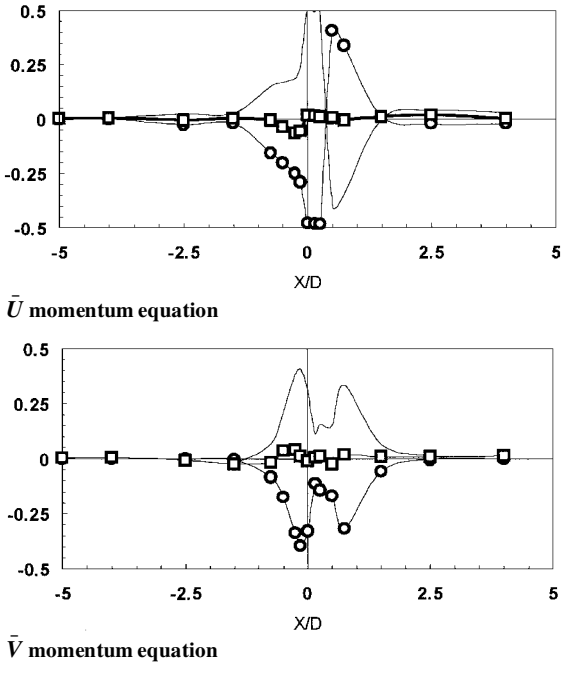

Fig. 4 Horizontal profiles of the convection (○), diffusion (□), and pressure (———) terms in the $\bar{U}$ and $\bar{V}$ momentum equations at $Y/D = 4.7$.

the impinging zone and significant regions where the sign is wrong were detected.

In spite of the failure of the k–ε turbulence model to predict the structure of the impinging zone, Barata et al.[1] also point out that the mean flow is reasonably well predicted because this type of flow is dominated by large pressure gradients. This can be explained with the help of Fig. 4, which presents the terms in the momentum equations obtained from the measurements. It shows that in the impingement region the diffusion term is negligible and the convection term is balanced by the pressure gradient term, as also observed for a low-Reynolds-number impinging jet without a crossflow (for example, see Ref. 6).

Conclusions

Budgets of turbulent kinetic energy are presented in the vicinity of the stagnation zone created by the impingement of a turbulent jet on a flat plate through a low-velocity crossflow.

Inspection of the terms in the conservation equation of the turbulent kinetic energy confirms that the turbulent structure of the flow in the ground vortex and impingement zones is associated with the interaction between normal stresses and normal strains. However, the mean flow can be reasonably well predicted using the k–ε turbulence model because the pressure gradient term in the momentum equations is dominant and is balanced by the convection term.

References

[1]Barata, J. M. M., Durão, D. F. G., Heitor, M. V., and McGuirk, J. J., "The Impingement of Single and Twin Turbulent Jets Through a Crossflow," *AIAA Journal*, Vol. 29, No. 4, 1991, pp. 595–602.

[2]Baker, O. J., "The Turbulent Horseshoe Vortex," *Journal of Wind Engineering and Industrial Aerodynamics*, Vol. 6, 1981, p. 9.

[3]Tennekees, H., and Lumley, J. L., *A First Course in Turbulence*, MIT Press, Cambridge, MA, 1972, p. 133.

[4]Castro, I. P., and Bradshaw, P., "The Structure of a Highly Curved Mixing Layer," *Journal of Fluid Mechanics*, Vol. 73, 1976, pp. 265–304.

[5]Chandrsuda, C., and Bradshaw, P., "Turbulence Structure of a Reattaching Mixing Layer," *Journal of Fluid Mechanics*, Vol. 110, 1981, pp. 171–194.

[6]Nishino, K., Samada, M., Kasuya, K., and Torii, K., "Turbulence Statistics in the Stagnation Region of an Axisymmetric Impinging Jet Flow," *International Journal of Heat and Fluid Flow*, Vol. 17, No. 3, 1996, pp. 193–201.

F. W. Chambers
Associate Editor

Mixing of Coaxial Jets with Small Annular Area in a Short Duct

S. D. Sharma* and M. R. Ahmed†
Indian Institute of Technology, Mumbai 400076, India

Nomenclature

C_p = coefficient of pressure, $(p - p_1)/0.5\rho U_m^2$
p = wall static pressure
p_1 = wall static pressure at the first station
r = radial coordinate
r_o = inner radius of the test section
U_m = mass-averaged velocity
u = streamwise mean velocity at a point
u' = rms value of streamwise velocity fluctuation
w' = rms value of transverse velocity fluctuation
x = axial (streamwise) coordinate
β = area ratio (outer to inner)
λ = velocity ratio (outer to inner)
ρ = air density
τ = nondimensional turbulence energy

Introduction

TURBULENT mixing of confined coaxial jets is a complex dynamic process that deserves a comprehensive investigation for deeper insight because it has many engineering applications. Several parameters contribute to this complexity, such as the diameter ratio of the jets, length-to-diameter ratio of the mixing duct, velocity ratio, density ratio, turbulence levels, etc. Unfortunately, information on the influence of each of these parameters still appears to be rather inadequate despite several prominent investigations that have been carried out to address the problem of the mixing of confined coaxial jets with varying conditions.[1–4] Although certain studies have contributed to the understanding of the mixing problems specific to gas turbine combustor applications with a sudden expansion[3,5] and introduction of swirl,[5–7] they have also added to the variety of the flow situation. Thus, a further widening of the scope for systematic research on the subject matter seems inevitable in view of the growing number of variables.

The present investigation deals with a particular case of mixing of coaxial jets in a nonseparating confinement with low annular-to-core-area ratio. The effect of two velocity ratios on mixing is examined for nearly a constant net mass flow rate.

Experimental Method

The experiments were carried out in a closed-circuit, all-steel wind tunnel consisting of two concentric contractions discharging airstreams with different velocities into the test section (a constant-diameter mixing duct) as shown in the inset to Fig. 1. The airflow was generated by two separate identical centrifugal blowers driven by two ac motors, each with 30-kW power. The return leg of the test rig opened into a plenum chamber that provided connections to the blower inlets. The airflow for the core stream was supplied through a settling chamber housing a perforated cone and a pair of stainless-steel wire screens serving as flow-straightening devices. Because no flow correction device was used for the annular stream, a relatively higher contraction ratio of 13.3 was employed for it against the contraction ratio of 7.4 for the core stream. The two coaxial airstreams were allowed to mix freely in the mixing duct having a length of 1000 mm and the same diameter as that of the outer jet of 380 mm. The inner jet diameter of 330 mm and its

Received Jan. 30, 1997; revision received May 27, 1998; accepted for publication June 9, 1998.

*Associate Professor, Department of Aerospace Engineering.
† Research Scholar, Department of Aerospace Engineering.

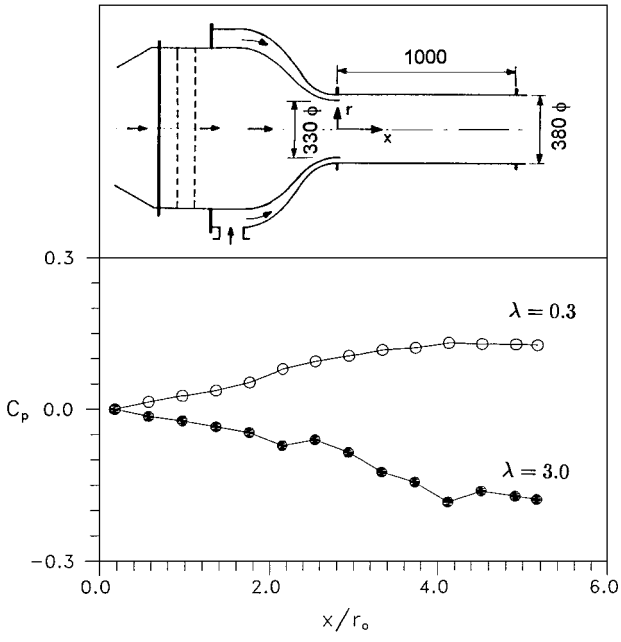

Fig. 1 Mixing duct wall pressure distribution.

nozzle (contraction) wall thickness of 5 mm left the annular gap of 20 mm at the entry to the mixing duct, thus providing the outer-jet-to-inner-jet-arearatio β of 0.26. A static frequency inverter was used to make the motor speed smoothly variable in the range of 5–100% of the rated speed. However, this static frequency inverter could be connected to only one of the two motors at a time, thus leaving the other motor running at the rated speed of 2800 rpm.

The experiments involved measurements of the mixing duct wall pressures, the mean velocity, and the turbulence intensities. The pressure distribution was obtained through equally spaced pressure taps of 0.5-mm diameter using a Furness Controls micromanometer, Model FC-0510, in conjunction with a multichannel box. Measurements of the mean velocity and the turbulence intensity were made with a 5-W argon-ion laser-based Dantec fiber-optic laser Doppler velocimetry (LDV) system operating in a single-component mode. Di-octyl pthalate particles, typically in the range of 1–2 μm, were introduced in the tunnel circuit as seed particles. The mixing duct was provided with an optical window all along its length. The LDV probe was traversed in a horizontal plane to accomplish measurements along the test section radius at several axial locations. A burst spectrum analyzer, Model 57N10, was used for processing the signal. Typically, 8000 samples were acquired at a point; however, the sample size was increased to 15,000 in regions of relatively high velocity gradient. Measurements of the mean transverse velocity component, performed at various locations including the high shear region, indicated that the flow had no detectable swirl.[8]

The motor speeds were adjusted such that the outer-to-inner-velocity ratios λ of 0.3 and 3.0 were obtained without changing the net mass flow rate. However, the jets being somewhat interdependent due to parallel connection of the blowers in the closed circuit, these inversely opposite velocity ratios of 0.3 and 3 could be obtained, respectively, at the mass-averaged velocities U_m of 30.8 and 31.3 m/s. The Reynolds number based on the mass-averaged velocity and the mixing duct diameter was calculated to be about 5.7×10^5. The LDV measurements in the nozzle wall boundary layers could not be made due to the practical difficulties involved in focusing the laser beams at those locations. Nonetheless, a pitot tube traverse indicated the boundary-layer thickness of about 2 mm on either side of the nozzle lip. The freestream turbulence levels of the inner and outer jets, measured close to the nozzle exit at $x/r_o = 0.12$ at the midradius of the jets, were 1.9 and 5.2% for $\lambda = 0.3$ and 1.7 and 4.2% for $\lambda = 3$, respectively.

The maximum error involved in the calculation of C_p was found to be 1.3%. Following Cenedese et al.,[9] the maximum error in the LDV measurement was found to be 0.4% for the mean velocity and 3.2% for the turbulence intensities. From the integration of measured velocity profiles at various streamwise stations, the conservation of mass was checked and was found to be within 1.7%.

Results and Discussion

Distribution of the mixing duct wall pressures along the flow direction is shown in nondimensional form in Fig. 1. For the lower velocity ratio $\lambda = 0.3$, a continuous rise in pressure with mild gradient is registered, whereas for $\lambda = 3$, the trend is the opposite. This is in agreement with the pressure variation reported in the initial mixing region by Razinsky and Brighton[1] and Choi et al.,[4] although the diameter ratio in their setup was much larger and they did not investigate the case for $\lambda > 1$. If the wall and wake effects are ignored, the pressure coefficient achieved on completion of the mixing can be determined from the momentum balance as follows:

$$C_p = \frac{2(\beta + 1)(\beta\lambda^2 + 1)}{(\beta\lambda + 1)^2} - 2 \tag{1}$$

Clearly, the velocity ratio and the area ratio, both in combination, will dictate a positive C_p value. Thus, the observed reversal of the pressure distribution with negative gradient for $\lambda = 3$ is surprising and was not expected. In fact, the pressure gradient was found to become substantially more negative with further increase in the velocity ratio.[8] These findings indicate a severe influence of smallness of the area ratio in terms of viscous losses arising from the strong interaction between the wall and the turbulent shear region in close proximity with increasingly vigorous mixing.

Figure 2 depicts profiles of nondimensional mean velocity, streamwise turbulence intensity, and transverse turbulence intensity.

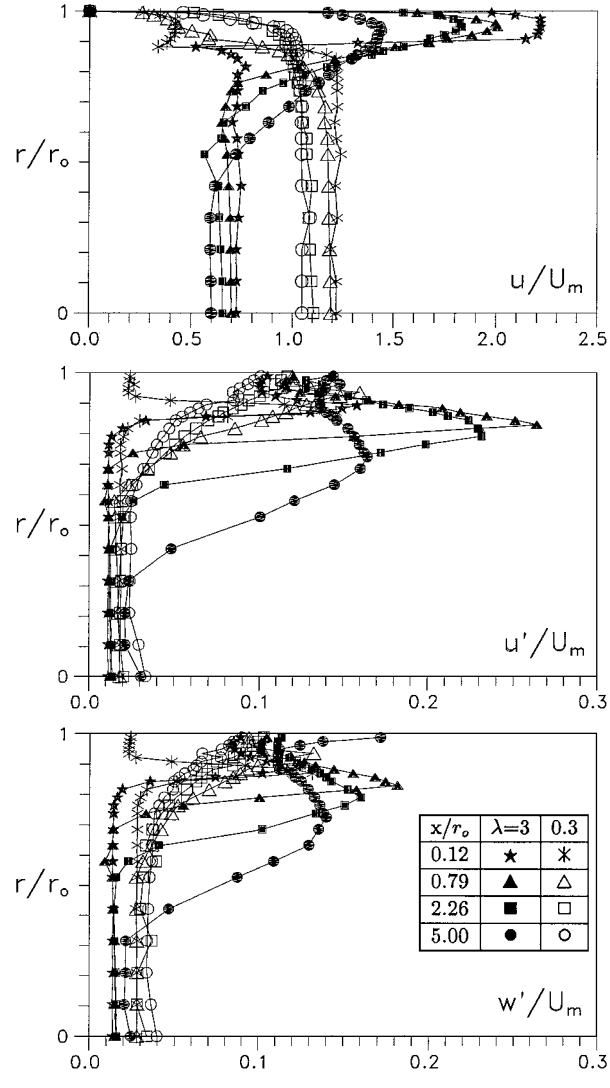

Fig. 2 Distribution of mean velocity, streamwise turbulence intensity, and transverse turbulence intensity.

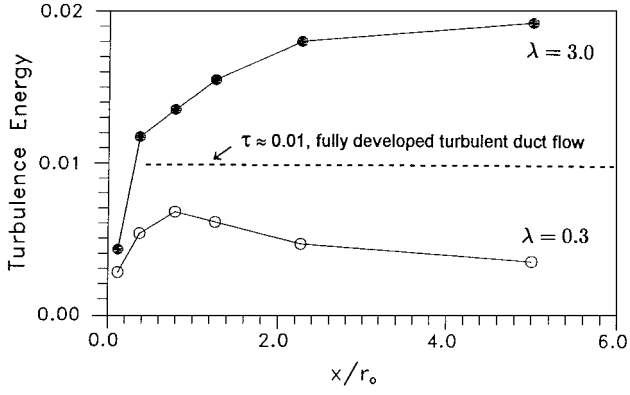

Fig. 3 Turbulence energy content in the mixing duct.

A sharp dip in the mean velocity profiles at the first measuring station ($x/r_o = 0.12$) illustrates a combined influence of the boundary layers and wake of the thick splitter plate in the formative region of the mixing layer. Mean velocity profiles for the subsequent stations indicate continuous exchange of momentum between the inner and the outer jets through the entrainment to the mixing layer. Consequently, the higher-velocity jet spreads into the region of the lower-velocity jet, and the velocity gradient between the two reduces. A striking feature of these plots is a nearly uniform decrease of about 14% for $\lambda = 0.3$ and about 17% for $\lambda = 3$ in the mean velocity between the first and the last measuring stations in the potential core region due to the entrainment effect. Because the annular gap in the present case is small, the spread of the core jet for $\lambda = 0.3$ in that region is spatially restricted by the duct, resulting in quick acceleration of the flow, as is evident from the velocity profile at $x/r_o = 5.0$. For $\lambda = 3.0$, the annular jet is required to penetrate a relatively large core area, and hence an appreciable velocity gradient is still seen to persist at $x/r_o = 5.0$; nevertheless, by then up to about 80% of the potential core is already consumed in the mixing process.

Distribution of the streamwise and transverse turbulence intensities at the first station, $x/r_o = 0.12$, clearly illustrates potential regions of the core and annular jets and the mixing layer. Nearly equal magnitudes of intensity of both of the turbulent components in potential regions indicate somewhat isotropic behavior and correspond to the respective freestream turbulence levels. As the flow develops at the subsequent measuring stations, the streamwise turbulence intensity becomes consistently higher compared with the transverse turbulence intensity, but their distribution is seen to retain similar characteristics: The magnitude of the turbulence peaks in the mixing layers initially increases and then decreases along with broadening of the peaks. This feature is more prominent for $\lambda = 3.0$ with effective spread toward the core axis. It is also noticed that the turbulence in the wall region grows steadily and eventually levels with the peak in the mixing region at the last measuring station. When collated with the results of Kulik et al.,[2] obtained for higher area and velocity ratios but for the same length-to-diameter-ratio mixing duct, the overall trends are found to bear appreciable similarity, indicating that the flow changes are more pronounced in and around the stream of smaller area. It is further understood that for confined mixing the momentum ratio of the two streams is more important as it incorporates the effect of area ratio.

Figure 3 shows the plots of nondimensional turbulence energy available across the cross-sectional area of the mixing duct along its length at various distances from the splitter plate trailing edge. The turbulence energy was computed from integration of the measured turbulence intensities, shown in Fig. 2, assuming that the third orthogonal component of turbulence (not measured) is equal to the transverse component. Thus the nondimensional total turbulence energy per unit mass in any radial plane is given by

$$\tau = \tfrac{1}{2}\left(u'^2/U_m^2\right) + \left(w'^2/U_m^2\right) \qquad (2)$$

For the velocity ratio $\lambda = 0.3$, the turbulence energy reaches its maximum quickly in the formative region and then continues to decay farther downstream, whereas for $\lambda = 3.0$, the rise in the turbulence energy is seen to build up monotonously, first rapidly and then at a gradually diminishing rate until the last measuring plane at $x/r_o = 5.0$. A value of turbulence energy that would be expected to approach asymptotically for a fully developed turbulent duct flow, $\tau \approx 0.01$, is also marked for the purpose of comparison of eventual convergence of the turbulence energy curves to this value. Thus, it appears that the mean flow will transfer energy to the turbulence components for the case when $\lambda = 0.3$, whereas the excess turbulence energy production due to strong interaction of the Reynolds stress with the mean shear for $\lambda = 3.0$ will be dissipated as the flow develops further. What is surmised from the limited test results for a geometry with low annular-to-core-arearatio is that the mixing between the coaxial streams occurs at the entrainment level for $\lambda < 1$, whereas it occurs at a finer scale for $\lambda > 1$. In the latter case, a more homogeneous mixture is expected due to intense turbulence promoting effective diffusion of the entrained mass.

Conclusions

The present experimental investigation on confined turbulent mixing has elicited certain characteristic features of a special case of coaxial ducted jets with low annular-to-core-area ratio for two different velocity ratios at nearly the same net mass flow rate. At the higher velocity ratio, the wall proximity effect becomes particularly pronounced, thereby resulting in 1) a significant pressure loss across the duct length contrary to the expected pressure rise due to mixing and 2) production of high turbulence that enables intense mixing to occur at fine scale.

Acknowledgments

Financial support for the work reported here was received from the sponsorship granted to the project Aero/RD-134/100/10/92/709 by the Aeronautics Research and Development Board, Ministry of Defence, Government of India. Thanks are due to F. W. Chambers of Oklahoma State University for his critical review of the manuscript.

References

[1]Razinsky, E., and Brighton, J. A., "Confined Jet Mixing for Non-Separating Conditions," *Journal of Basic Engineering*, Vol. 93, No. 3, 1971, pp. 333–349.

[2]Kulik, R. A., Leithem, J. J., and Weinstein, H., "Turbulence Measurements in a Ducted Co-Axial Flow," *AIAA Journal*, Vol. 8, No. 3, 1970, pp. 1694–1696.

[3]Johnson, B. V., and Bennett, J. C., "Statistical Characteristics of Velocity, Concentration, Mass Transport, and Momentum Transport for Co-Axial Jet Mixing in a Confined Duct," *Journal of Engineering for Gas Turbines and Power*, Vol. 106, Jan. 1984, pp. 121–126.

[4]Choi, B. W., Gessner, F. B., and Oates, G. C., "Measurements of Confined, Co-Axial Jet Mixing with Pressure Gradient," *Journal of Fluids Engineering*, Vol. 108, No. 1, 1986, pp. 39–46.

[5]Habib, M. A., and Whitelaw, J. H., "Velocity Characteristics of Confined Co-Axial Jets With and Without Swirl," *Journal of Fluids Engineering*, Vol. 102, No. 1, 1980, pp. 47–53.

[6]Ramos, J. I., and Sommer, H. T., "Swirling Flow in a Research Combustor," *AIAA Journal*, Vol. 23, No. 2, 1985, pp. 241–248.

[7]Gouldin, F. C., Depsky, J. S., and Lee, S. L., "Velocity Field Characteristics of a Swirling Flow Combustor," AIAA Paper 83-0314, Jan. 1983.

[8]Ahmed, M. R., "Experimental Investigation on Turbulent Mixing in Co-Axial, Confined Jets with Low Annular to Core Area Ratio," Ph.D. Thesis, Aerospace Engineering Dept., Indian Inst. of Technology, Bombay, India, Dec. 1997.

[9]Cenedese, A., Doglia, G., and Romano, G. P., "LDA and PIV Measurements in Free Jets," *Experimental Thermal and Fluid Science*, Vol. 9, No. 2, 1994, pp. 125–134.

F. W. Chambers
Associate Editor